

Laser-Induced Skyrmion Writing and Erasing in an Ultrafast Cryo-Lorentz Transmission Electron Microscope

G. Berruto,¹ I. Madan,¹ Y. Murooka,^{1,*} G. M. Vanacore,¹ E. Pomarico,¹ J. Rajeswari,¹
R. Lamb,² P. Huang,^{1,3} A. J. Kruchkov,³ Y. Togawa,^{2,4,5} T. LaGrange,⁶ D. McGrouther,²
H. M. Rønnow,³ and F. Carbone^{1,†}

¹*Institute of Physics, LUMES, École Polytechnique Fédérale de Lausanne (EPFL), Lausanne CH-1015, Switzerland*

²*Scottish Universities Physics Alliance, School of Physics and Astronomy, University of Glasgow, Glasgow G12 8QQ, United Kingdom*

³*Institute of Physics, LQM, École Polytechnique Fédérale de Lausanne (EPFL), Lausanne CH-1015, Switzerland*

⁴*Osaka Prefecture University, 1-2 Gakuencho, Sakai, Osaka 599-8570, Japan*

⁵*Chirality Research Center (CResCent), Hiroshima University, Higashi-Hiroshima, Hiroshima 739-8526, Japan*

⁶*Interdisciplinary Centre for Electron Microscopy, École Polytechnique Fédérale de Lausanne (EPFL), 1015 Lausanne, Switzerland*



(Received 15 September 2017; published 14 March 2018)

We demonstrate that light-induced heat pulses of different duration and energy can write Skyrmions in a broad range of temperatures and magnetic field in FeGe. Using a combination of camera-rate and pump-probe cryo-Lorentz transmission electron microscopy, we directly resolve the spatiotemporal evolution of the magnetization ensuing optical excitation. The Skyrmion lattice was found to maintain its structural properties during the laser-induced demagnetization, and its recovery to the initial state happened in the sub- μ s to μ s range, depending on the cooling rate of the system.

DOI: [10.1103/PhysRevLett.120.117201](https://doi.org/10.1103/PhysRevLett.120.117201)

Skyrmions are nanoscopic magnetic vortices with a nonzero topological charge. Creation, annihilation, and motion of Skyrmions in topological magnets offer interesting perspectives for spintronics and data storage devices [1,2]. While the former requires a simple and energy efficient way of manipulating the magnetic states, the latter aims at a fast and reliable way of writing, erasing and reading of individual Skyrmions or Skyrmion lattice segments in a confined volume. Furthermore, the study of the dynamics of the topological charge emergence introduces the concept of time into the physics of topological matter. Therefore, investigating the speed limit of Skyrmion creation and annihilation is paramount for both fundamental and applied perspectives.

In general, the rate of Skyrmions' appearance as well as their persistence range in the host material's phase diagram depend on the balance between thermodynamic and topological stability [3]. Significant advances have been achieved in the control and manipulation of Skyrmions in various hosting systems, ranging from insulating [4–8] to metallic [9–13], bulk and nanostructured helimagnets, to ultrathin heavy metals-ferromagnetic multilayered amorphous films [14–18]. Among them, the application of an electric field leads to the Skyrmion lattice rotation in insulating Cu_2OSeO_3 [4,7], and spin-transfer torque induced Skyrmion motion at ultralow current flow in metallic systems [9,10,12,16]. Alternately, short magnetic field pulses can lead to the appearance and precession of

Skyrmions and Skyrmion lattice segments [8,16,18], even employing ultrashort pulses, via the inverse Faraday effect [6]. However, to date spatially resolved information on the dynamical response of Skyrmions to time-varying stimuli and their intrinsic creation or annihilation speed is lacking. Such information, besides addressing the fundamental question of how fast Skyrmions can be created, is of pivotal importance for understanding the role of defects, edges, and nanostructuring on the control of Skyrmions. Furthermore, the creation or annihilation of Skyrmions solely by optical pulses has remained elusive so far and would provide a unique handle in magneto-optical devices.

In a recent body of work, magnetic bubbles [19,20] were photogenerated in thin films of ferrimagnetic rare earth-Fe-Co alloys [21–24] (See also Supplemental Material, note I [25]). Such magnetic textures are stabilized by uniaxial anisotropies and dipole-dipole interaction. The mechanism for their creation is based on the transient local heating above the Curie temperature [22,26,27] induced by a circularly polarized fs laser pulse [21–23]. Upon relaxation, the switched region defines the core of the magnetic bubble, and its size ($\approx 0.3 \mu\text{m}$ or larger [23]) and shape are determined by the beam profile and intensity.

Skyrmions in chiral magnets are fundamentally different from magnetic bubbles. They are stabilized by the competition between the magnetic exchange and the Dzyaloshinsky-Moriya (DM) interactions, and present a continuously whirling distribution of spins with a fixed chirality [2].

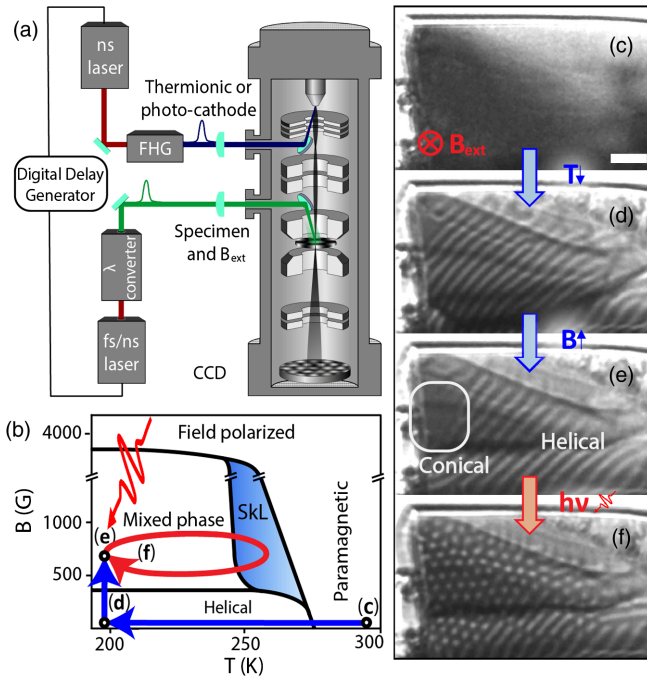


FIG. 1. Schematics of the Skyrmion photocreation. (a) Schematics of the experimental setup for *in situ* and pump-probe cryo-Lorentz microscopy. (b) Magnetic phase diagram of the FeGe nanoslab. Important paths in the phase diagram are drawn as arrows and discussed in the text. (c)–(f) Lorentz-Fresnel micrographs of the FeGe nanoslab, corresponding to the relative points in (b). The Skyrmion lattice in (f) is created by near-IR fs laser pulses. Scale bar is 250 nm.

Such a spatial texture can be dramatically confined (down to few nm), and is intrinsically determined by the properties of the host material.

Here, we report the generation and dynamical evolution of Skyrmions in the prototypical itinerant chiral magnet FeGe, initiated by laser-induced heat pulses. Contrary to the previously reported mechanisms [23,27,28], our approach allows the creation of Skyrmions without transiently reaching the paramagnetic state. Moreover, their size is independent on the laser beam diameter and fluence.

To determine the time needed for Skyrmions to be created or erased by laser pulses, we performed a combination of *in situ* cryo-Lorentz transmission electron microscopy (cryo-LTEM) and nanosecond (ns) pump-probe cryo-LTEM [29,30] [Fig. 1(a)]. The experiments were carried out in our modified JEOL JEM2100 TEM [31]. In this instrument, *in situ* cryo-LTEM can be performed in the Fresnel configuration [32] at camera-rate temporal resolution (ms) using a continuous wave electron beam generated thermoionically, upon *in situ* pulsed optical excitation of the specimen with tunable fs source (Supplemental Material, note II [25]).

Nanosecond time-resolved stroboscopic experiments were carried out in pump-probe mode. The ns electron probe pulses were photoemitted from a cathode exposed to a train of ultraviolet light pulses (4.66 eV). The delay with

respect to a train of visible light (2.33 eV) pump pulses illuminating the TEM sample was controlled via a digital delay generator. The laser spot size was kept at least 30 times larger than the sample lateral dimension, providing homogeneous illumination conditions.

The 60 nm thick FeGe sample was inserted in a liquid nitrogen cryogenic holder enabling temperature control between 100 and 300 K, and the external perpendicular magnetic field was controlled by variable objective lens excitation. The phase diagram of our nanoslab was determined by performing cryo-LTEM experiments at different temperatures and magnetic fields. A phase diagram sketch based on these experiments is depicted in Fig. 1(b).

The static temperature-dependent characterization [Figs. 1(c)–1(e)] of the magnetization pattern and the Skyrmion photocreation [Fig. 1(f)] were observed in cryo-LTEM in the Fresnel mode, using a nominal defocus length of 1400 nm. In the paramagnetic state, LTEM shows no magnetic contrast [Fig. 1(c)]. When cooled down below the Curie temperature, $T_C \approx 278$ K, in the minimum magnetic field achievable in our setup, 170 G, the material transforms to the helical phase, which is visible in LTEM as stripes [33]; see Fig. 1(d). At higher magnetic field and low temperature, the conical phase, which is indistinguishable from the field-polarized state in LTEM, is expected to be found based on previous experiments [34] and theoretical considerations [35]. In our sample, we observe either a coexistence of the conical and helical phase, or the Skyrmion phase, depending on the path followed in the phase diagram. The Skyrmion lattice (SkL) is a ground state in the narrow region of phase space visible in Fig. 1(b), above a characteristic field-dependent temperature $T_{\text{SkL}\uparrow}$ irrespective of the initial magnetic texture, and, once formed, was observed to persist upon field cooling down to the lowest temperature reachable in our setup, 100 K. In other words, the magnetic state of the sample in the “mixed phase” region of the phase diagram strongly depends on the field-dependent cooling or heating history, highlighting the hysteretic nature of the magnetic phases in FeGe. The initial state for the photocreation experiments was prepared via the path c-d-e depicted in Fig. 1(b), so that the sample was predominantly in the conical and helical phase [Fig. 1(e)], with no Skyrmion present.

From this region of the phase diagram, upon the *in situ* application of laser pulses, it is possible to write Skyrmions in the material; see Fig. 1(f) and supporting movies 1 and 2 in the Supplemental Material [25]. Skyrmions can then be fully erased by walking into the helical or field polarized phases and back, just by exciting the external magnetic field, at constant temperature. Large Skyrmion lattice segments can be also erased by high fluence optical pulses; see discussion below. We found that starting from 233 K, in a magnetic field of 400 G, a single 1.55 eV, 60 fs optical pulse of as little as 2 mJ/cm² is necessary to create a cluster of 10 to 14 Skyrmions. Given the typical Skyrmion

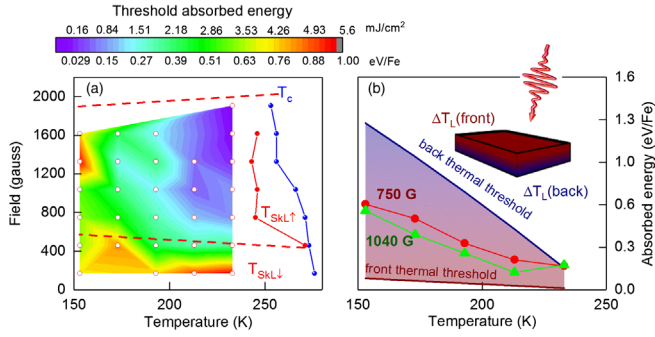


FIG. 2. Skyrmion photocreation phase diagram. (a) The color map encodes the Skyrmion photocreation energy threshold as a function of temperature and magnetic field; 60 fs long, linearly polarized 1.55 eV pulses were used. For comparison, the temperature $T_{SKL\uparrow}$ at which Skyrmions form upon field warming in absence of any photoexcitation and the critical temperature T_C for the Skyrmion to paramagnetic transition were measured experimentally and are shown as full symbols. The Skyrmion stability region after field cooling is enclosed between the red dashed lines $T_{SKL\downarrow}$. (b) Temperature dependence of the threshold at selected magnetic fields. For comparison, the fluence values required to warm up the lattice to $T_{SKL\uparrow}$ at the front (top) and back (bottom) surfaces of the sample are also shown, for $T_{SKL\uparrow} = 243$ K.

diameter of 70 nm, and the knowledge of FeGe optical absorption, a rough estimate of the optical energy expense is 8×10^{-15} J/Skyrmion, offering interesting perspectives for energy efficient data storage [36,37].

To determine the mechanism for the light-induced Skyrmion writing, we measured a fluence-dependence series and identified the energy per pulse necessary to create Skyrmions starting from the different positions in the phase diagram, indicated by open circles in Fig. 2(a). We estimated the threshold value by observing the magnetic pattern and gradually increasing the laser illumination fluence. The critical fluence is taken as the value to create well defined Skyrmions, and its error bar (approximately 18%) is estimated by repeating the same experiment 3 times. The distribution of threshold values obtained for the different sample conditions is plotted as a color map in Fig. 2(a).

As visible, at lower temperatures a larger energy is required to create Skyrmions, suggesting that the light-induced temperature rise in the material is responsible for their appearance. To test this hypothesis, we calculated the optical energy needed to cross $T_{SKL\uparrow}$ as a function of the starting temperature for both the top and bottom surfaces of the sample (Supplemental Material [25], note II, which includes Refs. [38,39]). These values are represented as solid red and blue lines in Fig. 2(b), respectively. The measured absorbed laser energy threshold values as a function of the starting temperature for a magnetic field of $B = 750$ and $B = 1040$ G are also displayed as red and green symbols, respectively. The experimental laser energy absorbed by the sample required to create Skyrmions

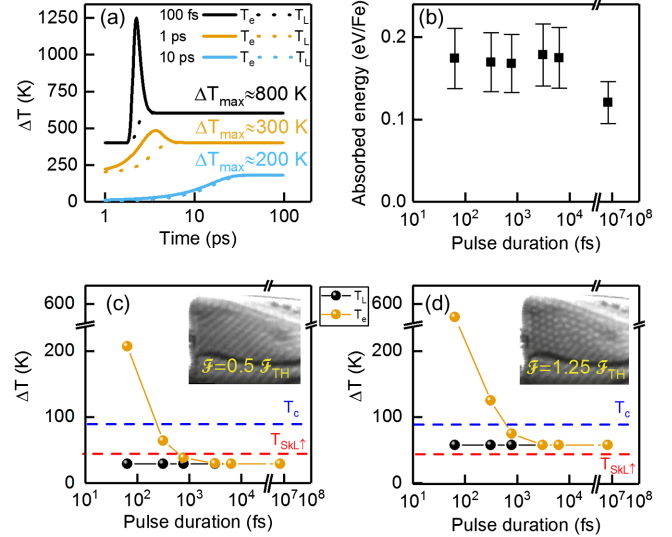


FIG. 3. Electron and lattice temperature evolution. (a) Two-temperature model calculations for three pulse durations, 100 fs, 1 ps, and 10 ps at the surface of the sample (solid and dashed lines for electronic and lattice temperatures, respectively). (b) Absorbed energy threshold for Skyrmions' photocreation as a function of pulse duration. (c),(d) Depth-averaged electronic and lattice temperature peaks as a function of pulse duration at one-half and just above the threshold fluence values. Red and blue dashed lines indicate temperature variation required to reach $T_{SKL\uparrow}$ and T_C upon field warming. The insets show the cryo-LTEM images taken upon photoexcitation of the sample at 233 K with 1.55 eV, 60 fs laser pulses.

largely exceeds the theoretical value for the top surface and lies somewhat below the value for the bottom surface, suggesting that sufficiently thick portions of the slab surpass the critical temperature to induce the Skyrmions formation.

Importantly, the electronic and lattice temperature follow a different dynamical evolution upon excitation by fast laser pulses. The light predominantly couples to the electronic subsystem resulting in a transient increase of the electronic temperature. The equilibration of the electronic and structural subsystems is mediated by the electron-phonon coupling and can be described by a two-temperature model (2TM) [40], see Supplemental Material, note II [25]. Typically, the shorter the light pulses, the higher the electronic temperature, and the larger its difference to the lattice temperature at the early stage of the dynamics. Such a behavior is depicted in Fig. 3(a), where the temporal evolution of the electronic and lattice temperature was obtained via the 2TM as a function of pulse duration.

To disentangle the role of these two subsystems, we performed a series of Skyrmion photocreation threshold measurements as a function of the pulse duration, Fig. 3(b). It is evident that the threshold is independent of the laser pulse duration, suggesting that the photoinduced electronic temperature jump does not play a role in the formation of the Skyrmions. To corroborate this idea, we show the

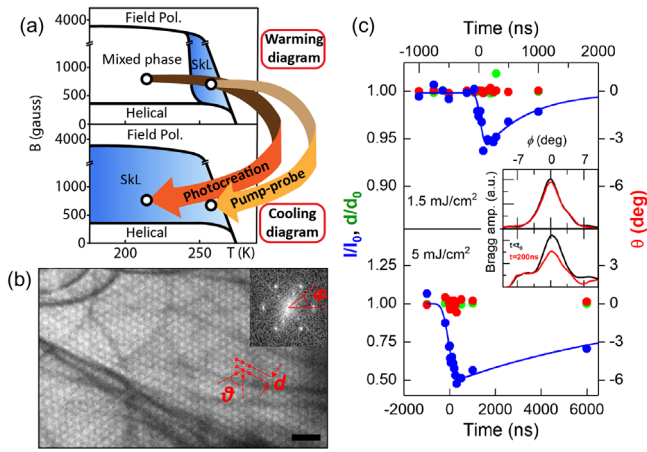


FIG. 4. ns pump-probe Lorentz TEM on Skyrmions. (a) Schematic evolution of the system across the phase diagram during the laser-writing (photocreation) and pump-probe experiments. (b) Portion of the Skyrmion lattice micrograph recorded with 25 ns photoelectron pulses and its Fourier transform, inset. Scale bar is 250 nm. (c) Pump-probe temporal dynamics of the Skyrmion lattice parameters: Skyrmion-Skyrmion distance (d/d_0 , green dots, left axis), orientation angle (red dots, right axis) and magnetization strength (I/I_0 , blue dots, left axis) at approximately 1.5 and 5 mJ/cm² fluence, top and bottom panel, respectively. The solid blue curves are fits to the magnetization strength via a finite rise-time exponential relaxation function, yielding recovery time constants of $0.75 \pm 0.3 \mu\text{s}$ at 1.5 mJ/cm², and $9.3 \pm 4.4 \mu\text{s}$ at 5 mJ/cm². The insets show the magnetic Bragg peak profile before the arrival of the pump pulse (black) and after 200 ns (red). The curves were obtained averaging over all six Bragg peaks after having verified that all have the same dynamics, ruling out distortions of the Skyrmion lattice.

photoinduced electronic and lattice temperature jump for different laser pulse durations above and below the threshold for photogenerating Skyrmions, Figs. 3(c) and 3(d). When only the electronic temperature far exceeds the critical value $T_{\text{SKL}\uparrow}$, no effect is observed on the magnetic pattern; conversely, if the lattice temperature is above $T_{\text{SKL}\uparrow}$, Skyrmions are observed in the sample. The threshold for the photogeneration of Skyrmions is also independent on the photon energy between 0.8 and 1.55 eV (see Supplemental Material, Fig. 1). This is expected for a thermally induced phenomenon considering the rather featureless optical conductivity of FeGe in such an energy range [41].

The fact that a very large electronic temperature does not result in observable changes of the system's magnetization, together with the insensitivity of the threshold to the driving pulses duration and wavelength, implies that the mechanism for creating Skyrmions is a slow process. In the single-pulse writing experiments, the phase diagram after the excitation is changed into the cooling phase diagram, see Fig. 4(a) red arrow, following an evolution similar to supercooling [42,43]. The sudden quench of thermal fluctuations ($\sim\text{K}/\mu\text{s}$) that takes place after the initial

temperature jump freezes Skyrmions in regions of the phase diagram where they were not present before the arrival of the laser pulse. This is consistent with previous reports showing that fast cooling rates, in the range of K/s, can homogeneously freeze-in Skyrmions in different regions of the phase diagram [44]. Importantly, in our case, the Skyrmion creation occurs in the limited region of the sample either close to an edge or at the interface between magnetic phases, while the majority of the sample conserves its magnetic state (see Supplemental Material, movies 1 and 2 [25]). This is different from the slower equilibrium-cooling experiments when most of the sample converts into the Skyrmion lattice, and showcases the role of the cooling rate in tipping the balance between topological protection and thermal fluctuations. In fact, the emergence of the Skyrmions is expected to happen at the edges of the sample where such a balance is altered by the breaking of topological protection. This has been experimentally observed upon magnetic field variation [45] and rationalized theoretically for the pulsed suppression of the magnetization [46].

To test the reaction speed of the sample's magnetization to a sudden temperature jump, we performed a ns pump-probe experiment in proximity of the Skyrmion to paramagnetic phase transition, Fig. 4(a) orange arrow, employing 20 kHz synchronized trains of laser and electron pulses, see Supplemental Material, note II [25]. We have chosen to study stroboscopically this transition because it is fully reversible when crossed at the slow rate of $<\text{K/s}$, and does not involve any metastable state (see Supplemental Material, Fig. 3 [25]). The FeGe slab was kept at 257 K and 950 G.

A portion of a typical Lorentz micrograph of the Skyrmion lattice recorded with photoelectrons is depicted in Fig. 4(b), together with its spatial Fourier Transform in the inset. The temporal evolution of the Skyrmion lattice constant, orientation angle, and magnetization strength for two fluences (approximately 1.5 and 5 mJ/cm²) are plotted in Fig. 4(c) top and bottom panels, respectively. We found no significant modification to either the Skyrmion lattice constant or its orientation angle. As the Skyrmion lattice constant is given by the ratio between the Dzyaloshinsky-Moriya D and the exchange constant J ($d = 4\pi J/|D|$), and the two are independent physical quantities, it is reasonable to conclude that neither D nor J are affected by the laser pulses on the ns time scale. Contrary, the intensity of the magnetic contrast, estimated as the intensity of the magnetic Bragg peak obtained by Fourier transforming the real-space image, is found to decrease by 6 and 49 percent for 1.5 and 5 mJ/cm² fluence, respectively. The time scale for the recovery of the magnetization depends on the fluence and reaches $\sim 9 \mu\text{s}$ for the strongest photoexcitation tested (5 mJ/cm²), confirming the idea that the magnetization dynamics is governed by the heat diffusion.

We can now further understand the writing process. After the photon absorption, the energy is transferred to the lattice on the few-ps time scale. The consequent excitation of magnetic fluctuations favors the Skyrmion creation at the sample edges and magnetic phase boundaries as long as $T > T_{\text{SKL}\uparrow}$. After $\sim 1 \mu\text{s}$, the system supercools down into the region of the phase diagram ($T < T_{\text{SKL}\uparrow}$) where the magnetization does not further evolve. Since we only observe the formation of up to 14 Skyrmions with each pulse and the optically written Skyrmion lattice is highly disordered [compare Figs. 1(f) and 4(b)], we can claim that few μs are not sufficient for establishing long-range Skyrmionic order, and Skyrmions are formed as individual self-assembling entities.

To corroborate this idea, we also performed an experiment where a single high-fluence pulse ($> 2.5 \times \mathcal{F}_{\text{TH}}$) was applied to the sample in which the Skyrmion lattice was already photoinduced (Supplemental Material, Fig. S2b [25]). At this photoexcitation level, the sample transient temperature exceeds T_C , resulting in its complete demagnetization. As a consequence, a large portion of the Skyrmion lattice disappears, and only few Skyrmions reform during cooling close to the edge of the specimen, see Fig. S2c [25]. The Skyrmion cluster size does not grow with the number of pulses and its position and shape differ after each individual laser pulse, confirming that each time the Skyrmion formation starts from the (transient) paramagnetic state.

In summary, we have shown that Skyrmions can be written in a FeGe nanoslab via illumination with optical pulses of different colors and duration. Our space-time resolved observations highlighted that the light-induced formation of Skyrmions takes place at the boundaries between magnetic domains and in proximity of the sample edges. The writing and erasing speed of the Skyrmions was found to be governed by the cooling rate following the laser-induced temperature jump. In the present case, the speed limitation is a direct consequence of the heat diffusion rate ($\text{K}/\mu\text{s}$) in our nanofabricated slab.

Based on our results, we suggest that increasing the cooling rate up to K/ps by connecting the sample to a heat-bath should result in the efficient Skyrmion optical erasing by strong ps pulses. The writing process would still be done by long ns pulses, whose pulse duration determines the thermalization time. The control of the Skyrmion cluster size could be attained by varying the duration of the writing pulse.

Furthermore, the modulation of the topological landscape via nanofabrication would also allow us to tune the creation and annihilation speed of the Skyrmions and their stability against external perturbations. A different behavior may be expected in nonmetallic Skyrmion hosts where the optical absorption can exhibit large energy gaps and light-induced excitations can have longer lifetimes. In such systems, also electronic effects may influence the fast dynamics of the Skyrmions.

The LUMES laboratory acknowledges support from the NCCR MUST, Sinergia CDSII5-171003 NanoSkyrmionics and an Ambizione grant of the Swiss National Science Foundation. G. B. acknowledges financial support from the Swiss National Science Foundation (SNSF) through the Grant No. 200021_159219/1. E. P. acknowledges financial support from the SNSF through an Advanced Postdoc Mobility Grant No. (P300P2_158473). H. M. R. acknowledges support from the SNSF through Grant No. 200020_166298. The authors would like to acknowledge M. Miyagawa, Y. Kousaka, T. Koyama, J. Akimitsu, and K. Inoue for the preparation and characterization of the bulk FeGe crystal, D. Demurtas, M. Cantoni, and D. Alexander from CIME for technical support with the cryogenic holder, A. Rosch, and A. Bogdanov, for insightful discussions, T. T. L. Lummen and A. Pogrebna for help with the setup and the experiments, respectively.

G. B. and I. M. contributed equally to this work.

*Present address: Ernst Ruska-Centre for Microscopy and Spectroscopy with Electrons and Peter Grünberg Institute, Forschungszentrum Jülich, 52425 Jülich, Germany.

†Corresponding author.

fabrizio.carbone@epfl.ch

- [1] A. Fert, V. Cros, and J. Sampaio, *Nat. Nanotechnol.* **8**, 152 (2013).
- [2] N. Nagaosa and Y. Tokura, *Nat. Nanotechnol.* **8**, 899 (2013).
- [3] H. Oike, A. Kikkawa, N. Kanazawa, Y. Taguchi, M. Kawasaki, Y. Tokura, and F. Kagawa, *Nat. Phys.* **12**, 62 (2015).
- [4] J. S. White *et al.*, *Phys. Rev. Lett.* **113**, 107203 (2014).
- [5] M. Mochizuki, X. Z. Yu, S. Seki, N. Kanazawa, W. Koshibae, J. Zang, M. Mostovoy, Y. Tokura, and N. Nagaosa, *Nat. Mater.* **13**, 241 (2014).
- [6] N. Ogawa, S. Seki, and Y. Tokura, *Sci. Rep.* **5**, 9552 (2015).
- [7] J. S. White *et al.*, *J. Phys. Condens. Matter* **24**, 432201 (2012).
- [8] Y. Onose, Y. Okamura, S. Seki, S. Ishiwata, and Y. Tokura, *Phys. Rev. Lett.* **109**, 037603 (2012).
- [9] T. Schulz, R. Ritz, A. Bauer, M. Halder, M. Wagner, C. Franz, C. Pfleiderer, K. Everschor, M. Garst, and A. Rosch, *Nat. Phys.* **8**, 301 (2012).
- [10] X. Z. Yu, N. Kanazawa, W. Z. Zhang, T. Nagai, T. Hara, K. Kimoto, Y. Matsui, Y. Onose, and Y. Tokura, *Nat. Commun.* **3**, 988 (2012).
- [11] S. Mühlbauer, B. Binz, F. Jonietz, C. Pfleiderer, A. Rosch, A. Neubauer, R. Georgii, and P. Boni, *Science* **323**, 915 (2009).
- [12] F. Jonietz *et al.*, *Science* **330**, 1648 (2010).
- [13] X. Z. Yu, N. Kanazawa, Y. Onose, K. Kimoto, W. Z. Zhang, S. Ishiwata, Y. Matsui, and Y. Tokura, *Nat. Mater.* **10**, 106 (2011).
- [14] P. Hsu, A. Kubetzka, A. Finco, N. Romming, K. von Bergmann, and R. Wiesendanger, *Nat. Nanotechnol.* **12**, 123 (2016).

- [15] M. Schott, A. Bernard-Mantel, L. Ranno, S. Pizzini, J. Vogel, H. Béa, C. Baraduc, S. Auffret, G. Gaudin, and D. Givord, *Nano Lett.* **17**, 3006 (2017).
- [16] S. Woo *et al.*, *Nat. Mater.* **15**, 501 (2016).
- [17] N. Romming, C. Hanneken, M. Menzel, J.E. Bickel, B. Wolter, K. von Bergmann, A. Kubetzka, and R. Wiesendanger, *Science* **341**, 636 (2013).
- [18] F. Büttner *et al.*, *Nat. Phys.* **11**, 225 (2015).
- [19] A. Fert, N. Reyren, and V. Cros, *Nat. Rev. Mater.* **2**, 17031 (2017).
- [20] N. S. Kiselev, A. N. Bogdanov, R. Schäfer, and U. K. Röbber, *Phys. Rev. Lett.* **107**, 179701 (2011).
- [21] C. D. Stanciu, F. Hansteen, A. V. Kimel, A. Kirilyuk, A. Tsukamoto, A. Itoh, and T. Rasing, *Phys. Rev. Lett.* **99**, 047601 (2007).
- [22] T. Ogasawara, N. Iwata, Y. Murakami, H. Okamoto, and Y. Tokura, *Appl. Phys. Lett.* **94**, 162507 (2009).
- [23] M. Finazzi, M. Savoini, A. R. Khorsand, A. Tsukamoto, A. Itoh, L. Duo, A. Kirilyuk, T. Rasing, and M. Ezawa, *Phys. Rev. Lett.* **110**, 177205 (2013).
- [24] A. Kirilyuk, A. V. Kimel, and Th. Rasing, *Rev. Mod. Phys.* **82**, 2731 (2010).
- [25] See Supplemental Material at <http://link.aps.org/supplemental/10.1103/PhysRevLett.120.117201> for a discussion on magnetic bubbles, a description of the experimental setup and methods, movies on Skyrmion photocreation, and figures of optical Skyrmion erasing.
- [26] A. R. Khorsand, M. Savoini, A. Kirilyuk, A. V. Kimel, A. Tsukamoto, A. Itoh, and Th. Rasing, *Phys. Rev. Lett.* **108**, 127205 (2012).
- [27] W. Koshibae and N. Nagaosa, *Nat. Commun.* **5**, 5148 (2014).
- [28] H. Fujita and M. Sato, *Phys. Rev. B* **95**, 054421 (2017).
- [29] H. S. Park, J. S. Baskin, and A. H. Zewail, *Nano Lett.* **10**, 3796 (2010).
- [30] K. B. Schliep, P. Quarterman, J. P. Wang, and D. J. Flannigan, *Appl. Phys. Lett.* **110**, 222404 (2017).
- [31] L. Piazza, D. J. Masiel, T. LaGrange, B. W. Reed, B. Barwick, and F. Carbone, *Chem. Phys.* **423**, 79 (2013).
- [32] S. McVitie and M. Cushley, *Ultramicroscopy* **106**, 423 (2006).
- [33] M. Uchida, Y. Onose, Y. Matsui, and Y. Tokura, *Science* **311**, 359 (2006).
- [34] A. O. Leonov *et al.*, *Phys. Rev. Lett.* **117**, 087202 (2016).
- [35] M. N. Wilson, A. B. Butenko, A. N. Bogdanov, and T. L. Monchesky, *Phys. Rev. B* **89**, 094411 (2014).
- [36] A. Rosch, *Nat. Nanotechnol.* **12**, 103 (2017).
- [37] A. Rosch, *Nat. Nanotechnol.* **8**, 160 (2013).
- [38] H. Wilhelm, A. O. Leonov, U. K. Röbber, P. Burger, F. Hardy, C. Meingast, M. E. Gruner, W. Schnelle, M. Schmidt, and M. Baenitz, *Phys. Rev. B* **94**, 144424 (2016).
- [39] N. A. Porter, J. C. Gartside, and C. H. Marrows, *Phys. Rev. B* **90**, 024403 (2014).
- [40] P. B. Allen, *Phys. Rev. Lett.* **59**, 1460 (1987).
- [41] V. Guritanu, D. van der Marel, J. Teyssier, T. Jarlborg, H. Wilhelm, M. Schmidt, and F. Steglich, *Phys. Rev. B* **75**, 155114 (2007).
- [42] K. Karube *et al.*, *Nat. Mater.* **15**, 1237 (2016).
- [43] T. Eggebrecht, M. Möller, J. G. Gatzmann, N. Rubiano da Silva, A. Feist, U. Martens, H. Ulrichs, M. Münzenberg, C. Ropers, and S. Schäfer, *Phys. Rev. Lett.* **118**, 097203 (2017).
- [44] J. Wild *et al.*, *Sci. Adv.* **3**, e1701704 (2017).
- [45] H. Du *et al.*, *Nat. Commun.* **6**, 8504 (2015).
- [46] J. Müller, A. Rosch, and M. Garst, *New J. Phys.* **18**, 065006 (2016).